Slow Magnetic Relaxation in Luminescent Mononuclear Dysprosium(III) and Erbium(III) Pentanitrate Complexes with the Same LnO_{10} Coordination Geometry

*Lei Chen,[ab] JianJun Zhou,[b] Aihua Yuan,[*b] and You Song[*c]*

[a]*School of Material Science and Engineering, Jiangsu University of Science and Technology, Zhenjiang 212003, P. R. China*

[b]*School of Environmental and Chemical Engineering, Jiangsu University of Science and Technology, Zhenjiang 212003, P. R. China, E-mail: aihua.yuan@just.edu.cn*

[c]*State Key Laboratory of Coordination Chemistry, Nanjing National Laboratory of Microstructures, School of Chemistry and Chemical Engineering, Nanjing University, Nanjing 210093, P. R. China, E-mail: yousong@nju.edu.cn*

Electronic Supplementary Information

Table S1. Summary of crystal data and refinement for **1-Dy** and **2-Er**.

	1-Dy	**2-Er**
Molecular formula	$C_{32}H_{72}DyN_7O_{15}$	$C_{32}H_{72}ErN_7O_{15}$
CCDC no	1562706	1562707
Formula weight	957.47	962.21
Temperature	296(2) K	296(2) K
Wavelength / Å	0.71073	0.71073
crystal system	Monoclinic	Monoclinic
Space group	*P2(1)/c*	*P2(1)/c*
a / Å	14.4086(4)	14.427(6)
b / Å	16.7714(4)	16.805(6)
c / Å	20.7859(6)	20.761(8)
β / deg	107.319(2)	107.422(4)
V / Å^3	4795.2(2)	4803(3)
Z	4	4
D_{calc}, g/cm^3	1.326	1.331
μ / mm^{-1}	1.621	1.811
F (000)	1996	1996
Goodness-of-fit on F^2	1.119	1.069
Final R indices [$I > 2\sigma(I)$][a]	R_1 = 0.0498, wR_2 = 0.1099	R1 = 0.0551, wR2 = 0.1509
R indices (all data)[a]	R_1 = 0.1164, wR_2 = 0.1409	R1 = 0.1011, wR2 = 0.2039

[a]$wR_2 = [\Sigma[w(F_o^2-F_c^2)^2]/\Sigma[w(Fo^2)^2]]^{1/2}$, $R_1 = \Sigma||F_o|-|F_c||/\Sigma|F_o|$.

Table S2. Selected Bond Lengths (Å) and Angles (deg) for **1-Dy.**

Bond lengths (Å)		Angles (deg)	
Dy(1)-O(1)	2.434(6)	O(1)-Dy(1)-O(2)	49.13(19)
Dy(1)-O(2)	2.439(6)	O(4)-Dy(1)-O(5)	50.36(19)
Dy(1)-O(4)	2.433(5)	O(7)-Dy(1)-O(8)	51.1(2)
Dy(1)-O(5)	2.431(6)	O(10)-Dy(1)-O(11)	50.92(18)
Dy(1)-O(7)	2.453(5)	O(13)-Dy(1)-O(14)	51.87(18)
Dy(1)-O(8)	2.426(5)		
Dy(1)-O(10)	2.448(4)		
Dy(1)-O(11)	2.427(5)		
Dy(1)-O(13)	2.426(4)		
Dy(1)-O(14)	2.446(5)		

Table S3. Selected Bond Lengths (Å) and Angles (deg) for **2-Er**.

Bond lengths(Å)		Angles (deg)	
Er(1)-O(1)	2.404(8)	O(1)-Er(1)-O(2)	51.0(3)
Er(1)-O(2)	2.410(7)	O(4)-Er(1)-O(5)	51.5(3)
Er(1)-O(4)	2.387(8)	O(9)-Er(1)-O(7)	48.7(3)
Er(1)-O(5)	2.435(7)	O(10)-Er(1)-O(12)	50.9(3)
Er(1)-O(7)	2.428(9)	O(14)-Er(1)-O(13)	51.2(3)
Er(1)-O(9)	2.421(8)		
Er(1)-O(10)	2.393(6)		
Er(1)-O(12)	2.447(7)		
Er(1)-O(13)	2.445(8)		
Er(1)-O(14)	2.414(7)		

Table S4. The results of the continuous shape measure (CSM) analyses of $Ln(NO_3)_5^{2-}$ in **1-Dy** and **2-Er** by SHAPE software

Complex	*SDD (D2)	TD (C2v)	JBCSAPR (D4d)	JSPC (C2v)
1-Dy	2.268	1.546	6.630	3.816
2-Er	2.307	1.583	6.623	3.797

*SDD = Staggered Dodecahedron; TD = Tetradecahedron; JBCSAPR = Bicapped square antiprism; JSPC = Sphenocorona J87

Table S5. Crystal field parameters for **1-Dy** and **2-Er** fitted from $\chi_M T$ *vs.* T and M *vs.* H simultaneously.

	1	**2**
B_0^2	-249.1	-1174.4
B_0^4	269.5	915.6
B_2^4	125.2	170.6
B_4^4	365.9	-640.2

Table S6. Energy levels and eigenstates for **1-Dy** and **2-Er** fitted from $\chi_M T$ *vs.* T and M *vs.* H simultaneously.

	Energy / cm^{-1}	Eigenstate
1	0	0.41|±1/2>+0.31|±3/2>+0.18|±5/2>+0.07|±7/2>+0.02|±9/2>+…
	30	0.35|±1/2>+0.29|±3/2>+0.19|±5/2>+0.11|±7/2>+0.05|±9/2>+…
	100	0.57|±5/2>+0.32|±3/2>+0.04|±9/2>+0.03|±7/2>+…
	112	0.69|±7/2>+0.15|±9/2>+0.09|±1/2>+0.03|±3/2>+…
	151	0.73|±9/2>+0.15|±1/2>+0.07|±7/2>+…
	191	0.90|±11/2>+0.04|±3/2>+0.03|±7/2>+…
	248	0.96|±13/2>+0.03|±9/2>+…
	312	0.98|±15/2>+0.2|±11/2>+…
2	0	±11/2
	134	0.94|±9/2>+0.6|±13/2>
	215	0.94|±13/2>+0.06|±9/2>
	452	0.99|±7/2>+…
	802	0.97|±5/2>+0.03|±3/2>
	975	±15/2
	1117	0.96|±3/2>+0.03|±5/2>+…
	1277	0.99|±1/2>+…

Table S7. The parameters obtained by fitting Cole-Cole plot under 500 Oe dc field for **1-Dy**.

T / K	χ_S	χ_T	τ	a
1.8	1.23	4.85	0.00094	0.22
1.9	1.19	4.58	0.00069	0.19
2.0	1.11	4.35	0.00048	0.17
2.1	1.03	4.16	0.00033	0.15
2.2	0.86	4.00	0.00021	0.15
2.3	0.52	3.85	0.00012	0.16

Table S8. The parameters obtained by fitting Cole-Cole plot under 1000 Oe dc field for **2-Er**.

T / K	χ_S	χ_T	τ	a
1.8	0.18	3.49	0.00366	0.22
2.0	0.14	3.21	0.00273	0.22
2.2	0.13	2.95	0.00189	0.20
2.4	0.12	2.71	0.00121	0.17
2.6	0.13	2.51	0.00075	0.13
2.8	0.12	2.34	0.00046	0.10
3.0	0.09	2.21	0.00028	0.10
3.2	0.06	2.08	0.00017	0.08

Table S9. The parameters obtained by fitting Cole-Cole plot under 500 Oe dc field for **1-$Dy_{0.18}Y_{0.82}$**.

T / K	χ_S	χ_T	τ	a
1.8	0.021	0.16	0.00142	0.10
2.0	0.021	0.15	0.00058	0.07
2.2	0.020	0.14	0.00027	0.06

Table S10. The parameters obtained by fitting Cole-Cole plot under 1000 Oe dc field for **2-$Er_{0.13}Y_{0.87}$**.

T / K	χ_S	χ_T	τ	a
1.8	0.012	0.32	0.00841	0.10
2.0	0.014	0.31	0.00699	0.08
2.2	0.011	0.30	0.00586	0.10
2.4	0.013	0.28	0.00452	0.06
2.6	0.014	0.28	0.00380	0.06
2.8	0.013	0.25	0.00212	0.04
3.0	0.012	0.23	0.00115	0.03
3.5	0.011	0.22	0.00067	0.03

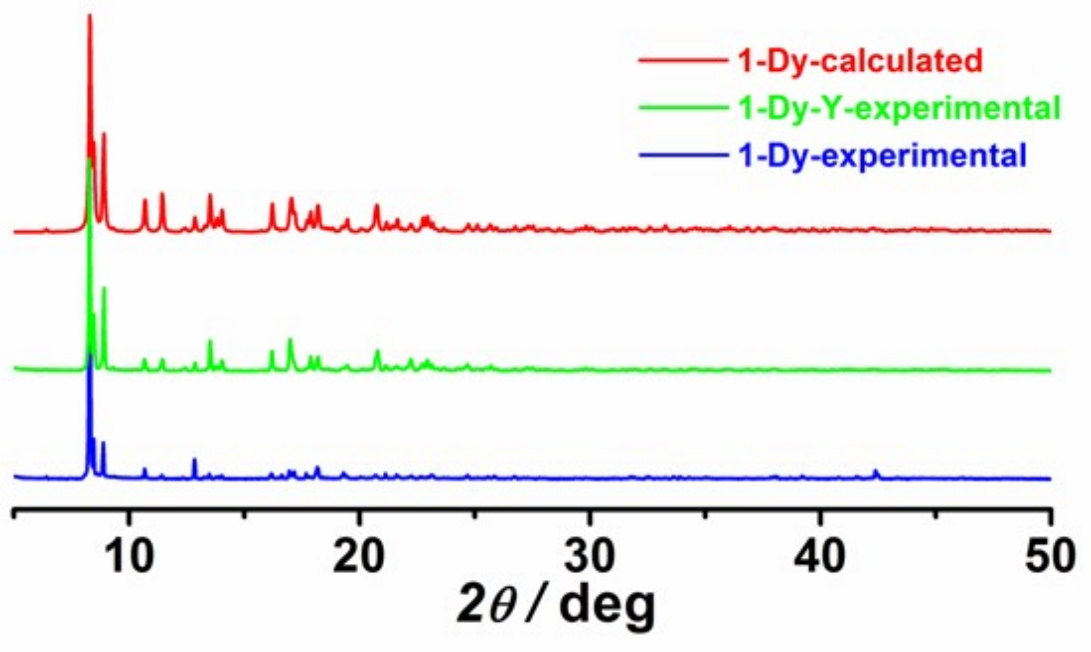

Figure S1. XRD patterns for complexes **1-Dy** and **1-Dy$_{0.18}$Y$_{0.82}$.**

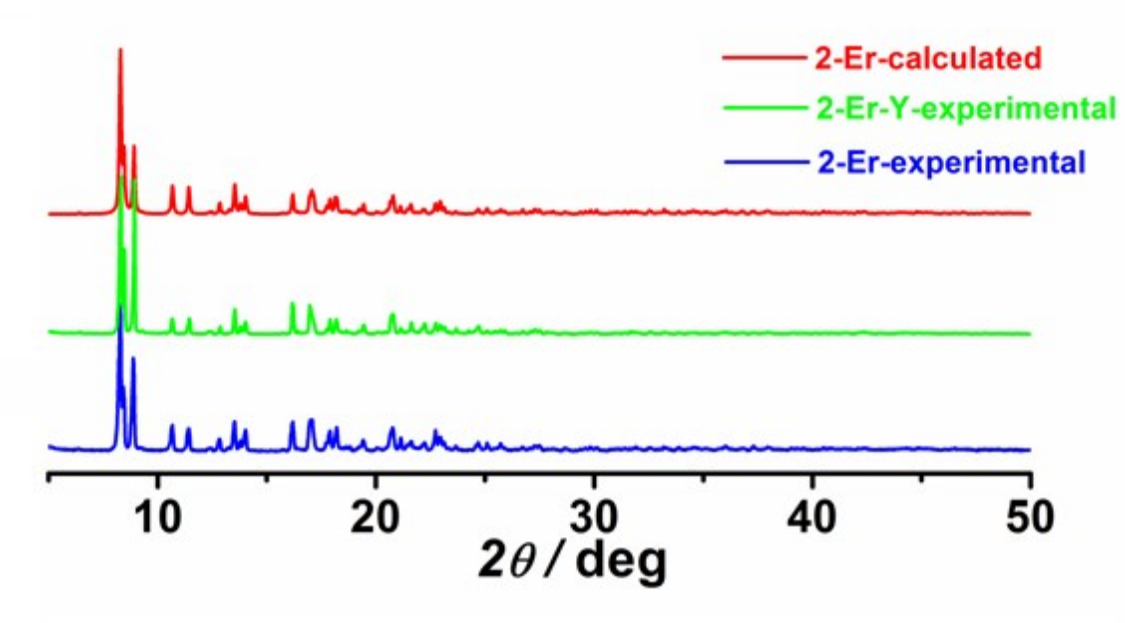

Figure S2. XRD patterns for complexes **2-Er** and **2-Er$_{0.13}$Y$_{0.87}$**.

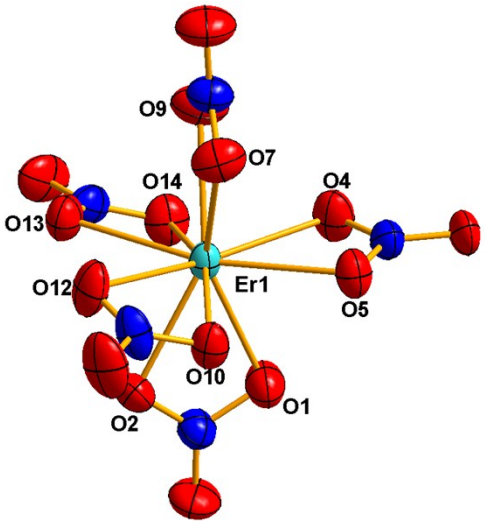

Figure S3. ORTEP drawing of the anion $[Er(NO_3)_5]^{2+}$ in **2-Er**. Cyan, red, and blue spheres represent Er, O, and N atoms, respectively. H atoms are omitted for clarity.

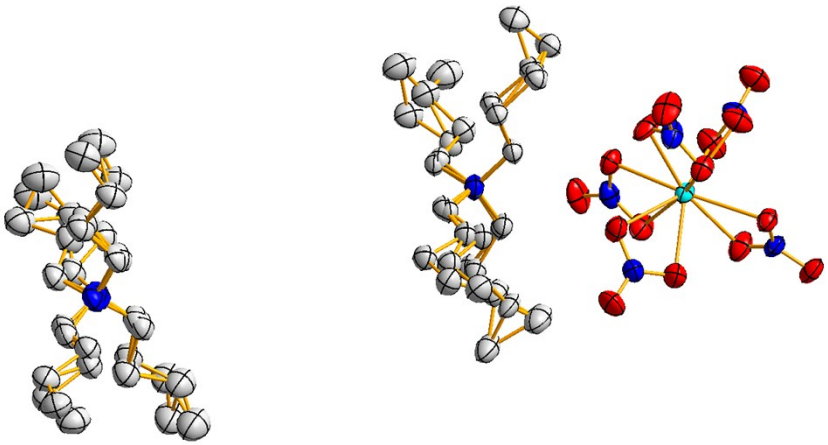

Figure S4. ORTEP drawing of the asymmetric unit in **1-Dy**. Cyan, red, blue, and gray spheres represent Dy, O, N and C atoms, respectively. H atoms are omitted for clarity.

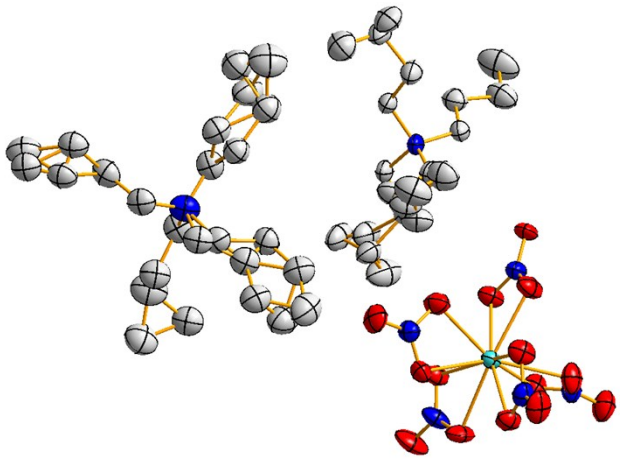

Figure S5. ORTEP drawing of the asymmetric unit in **2-Er**. Cyan, red, blue, and gray spheres represent Er, O, N and C atoms, respectively. H atoms are omitted for clarity.

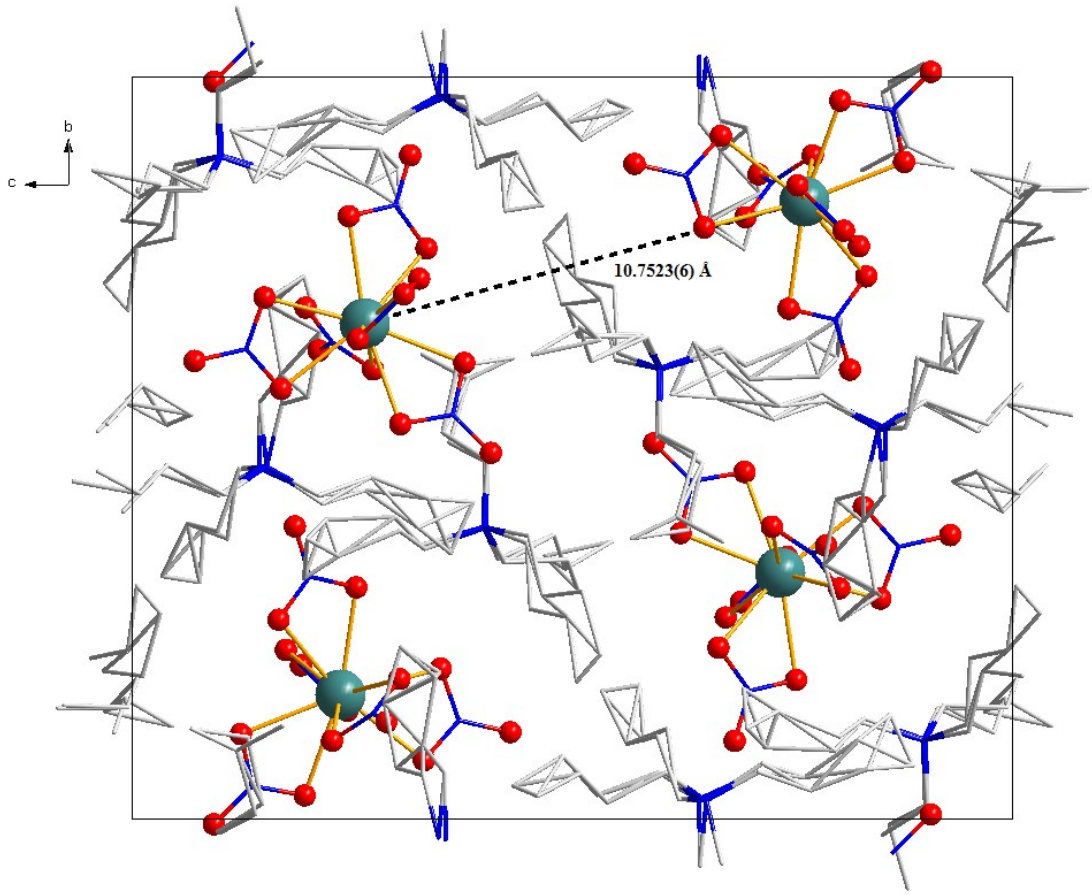

Figure S6. Crystal packing of **1-Dy** along the a axis. The H atoms are omitted for clarity.

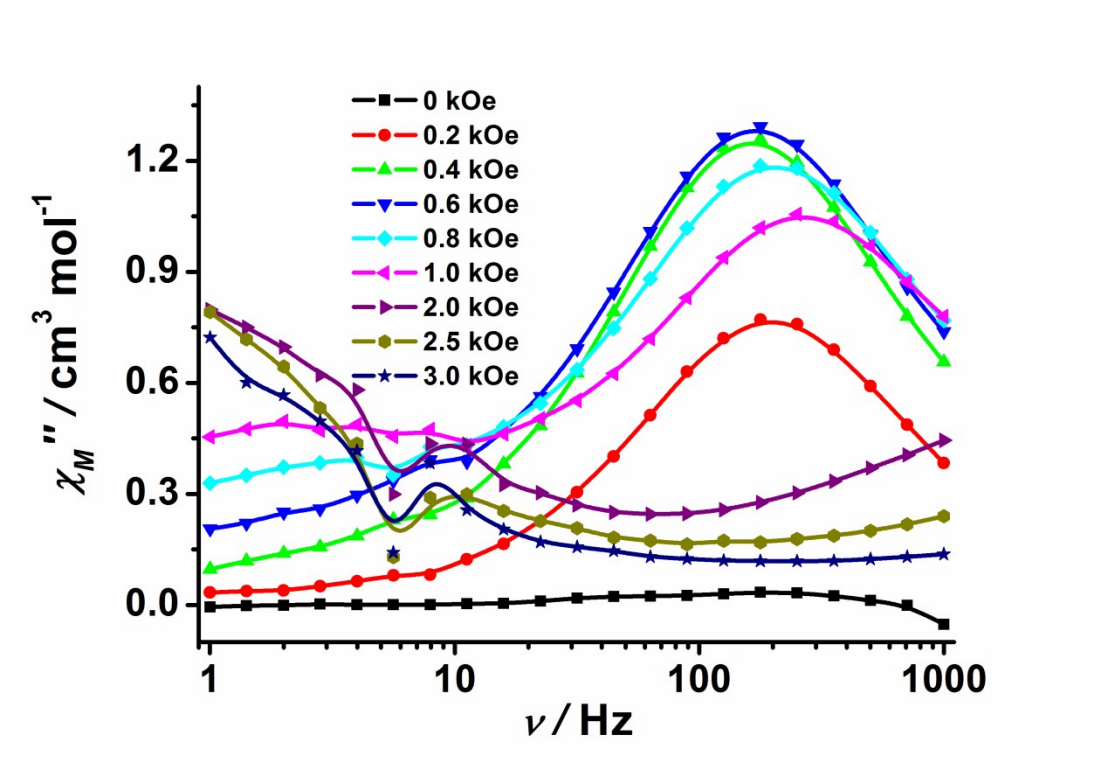

Figure S7. Frequency dependence of out-of-phase (χ_M'') ac susceptibility at 1.8 K under the different applied static fields from 0 to 3000 Oe for **1-Dy**. The solid lines are for eye guide.

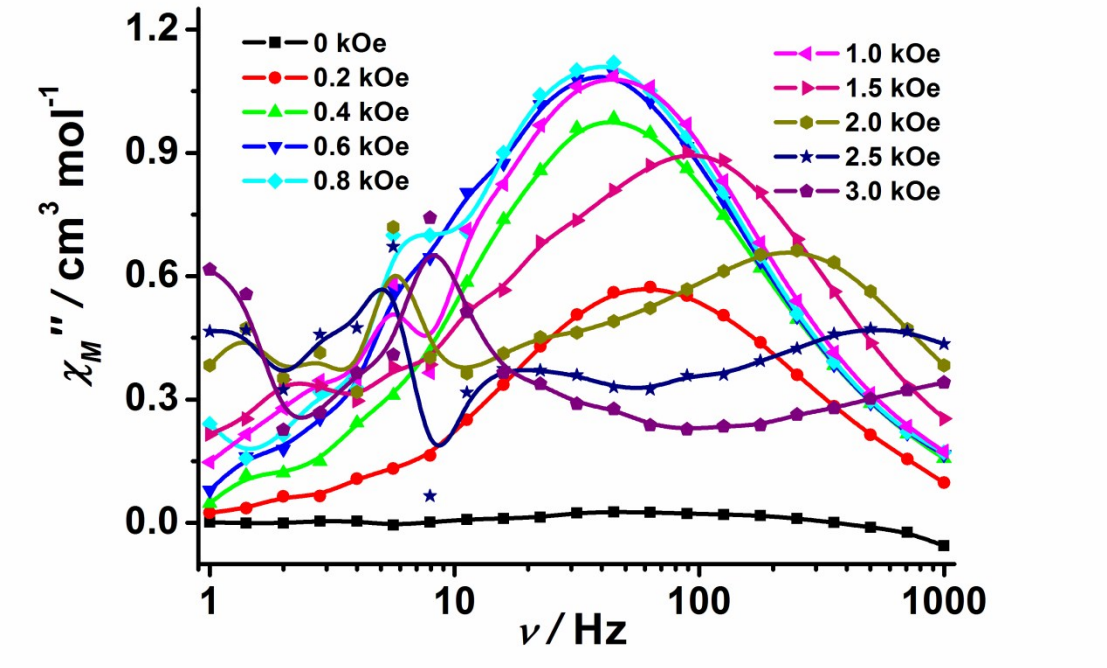

Figure S8. Frequency dependence of out-of-phase (χ_M'') ac susceptibility at 1.8 K under the different applied static fields from 0 to 3000 Oe for **2-Er**. The solid lines are for eye guide.

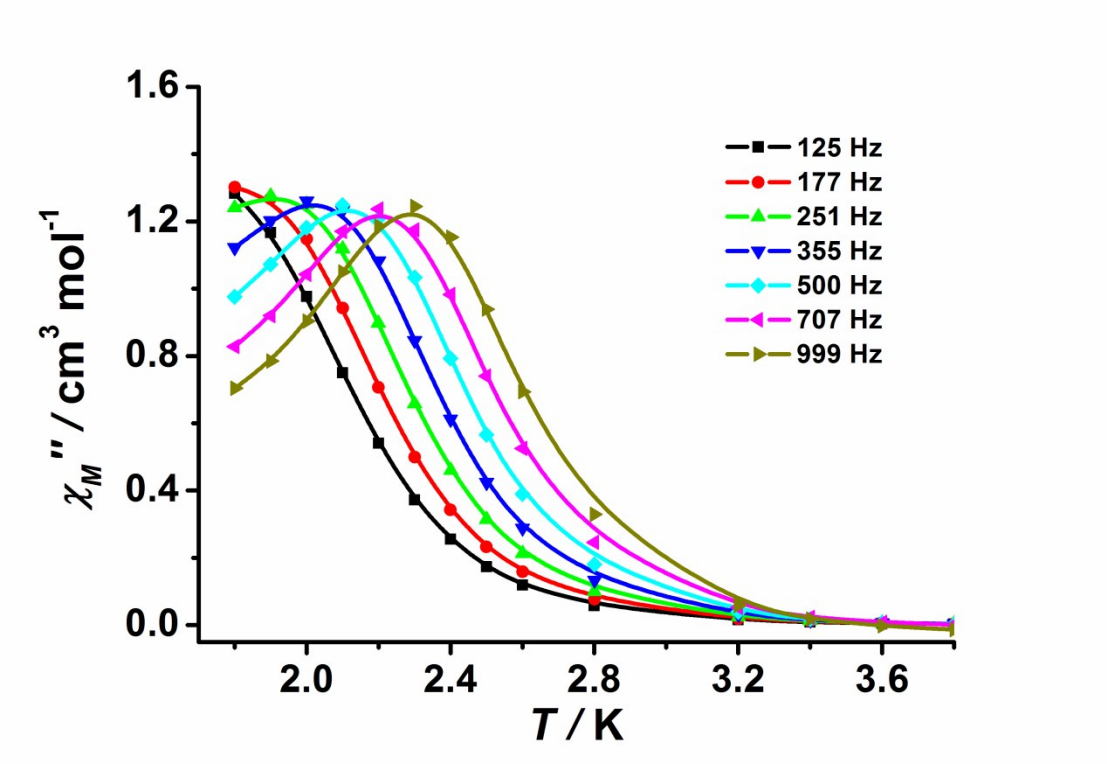

Figure S9. Temperature dependence of out-of-phase ac susceptibility (χ_M'') at different ac frequency under a 500 Oe dc field for **1-Dy**. The solid lines are for eye guide.

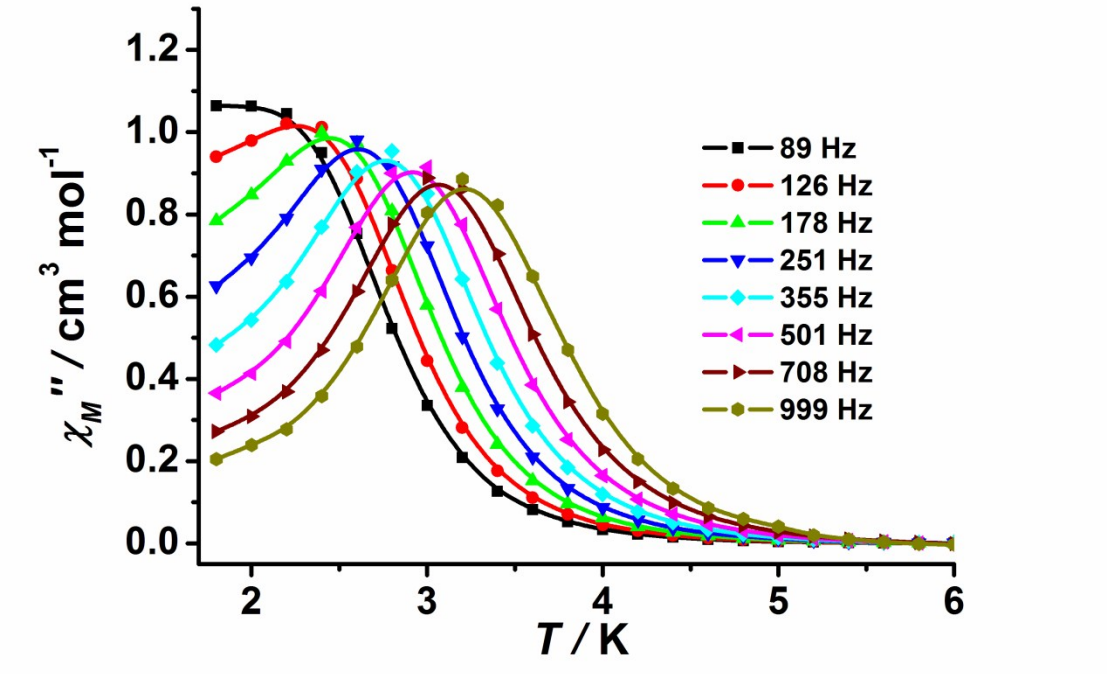

Figure S10. Temperature dependence of out-of-phase ac susceptibility (χ_M'') at different ac frequency under a 1000 Oe dc field for **2-Er**. The solid lines are for eye guide.

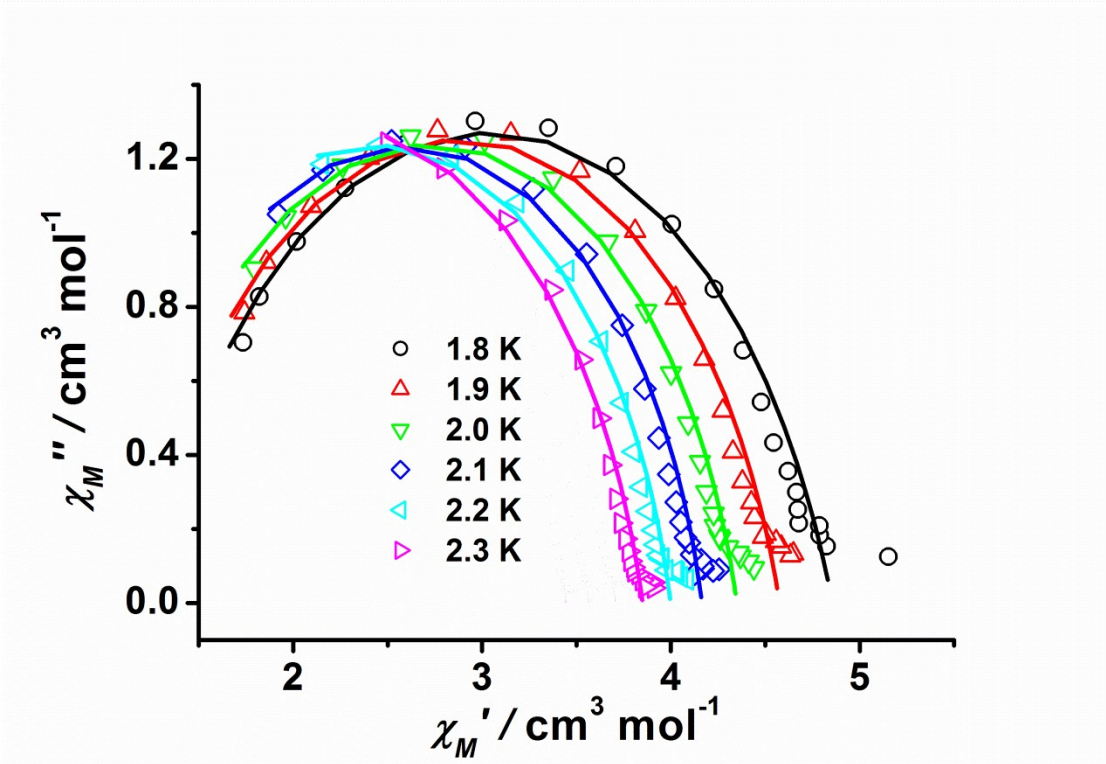

Figure S11. Cole-Cole plot obtained from the ac susceptibility data under a 500 Oe dc field in the temperature range of 1.8-2.3 K for **1-Dy**. Solid lines represent the best fits to a generalized Debye model.

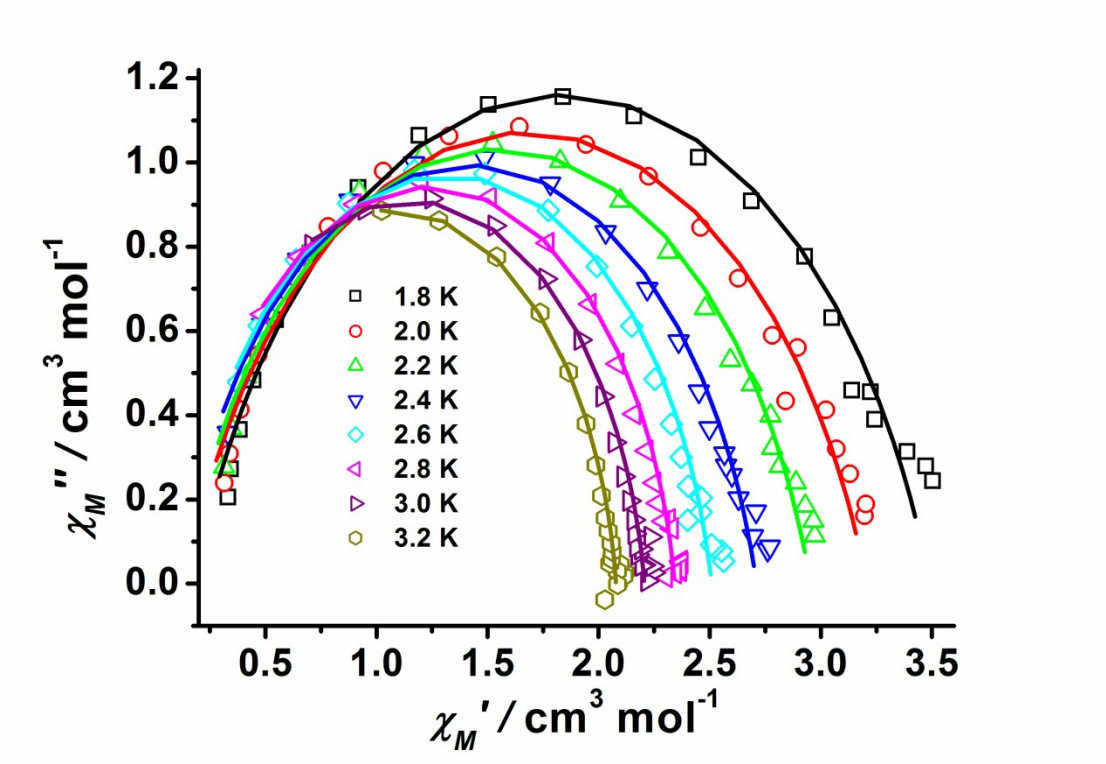

Figure S12. Cole-Cole plot obtained from the ac susceptibility data under a 1000 Oe dc field in the temperature range of 1.8-3.2 K for **2-Er**. Solid lines represent the best fits to a generalized Debye model.

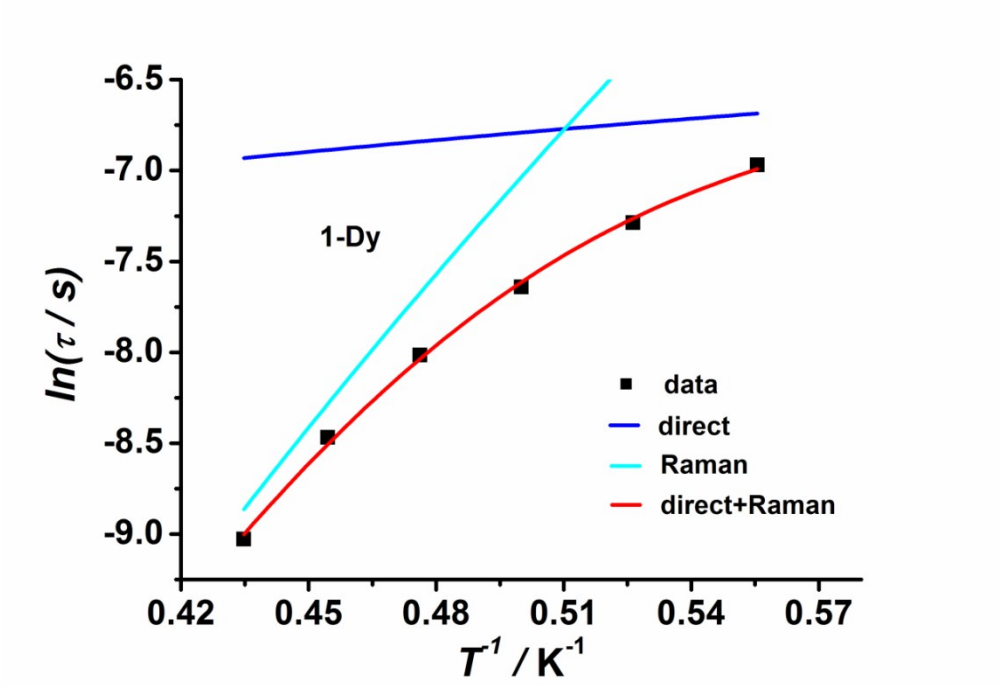

Figure S13. Temperature dependence of the magnetization relaxation rates of **1-Dy** under an applied dc field of 500 Oe. The solid red lines represent the best fit by using eq (2). The other solid lines represent data fits using individual direct (blue) and Raman (cyan) processes, respectively.

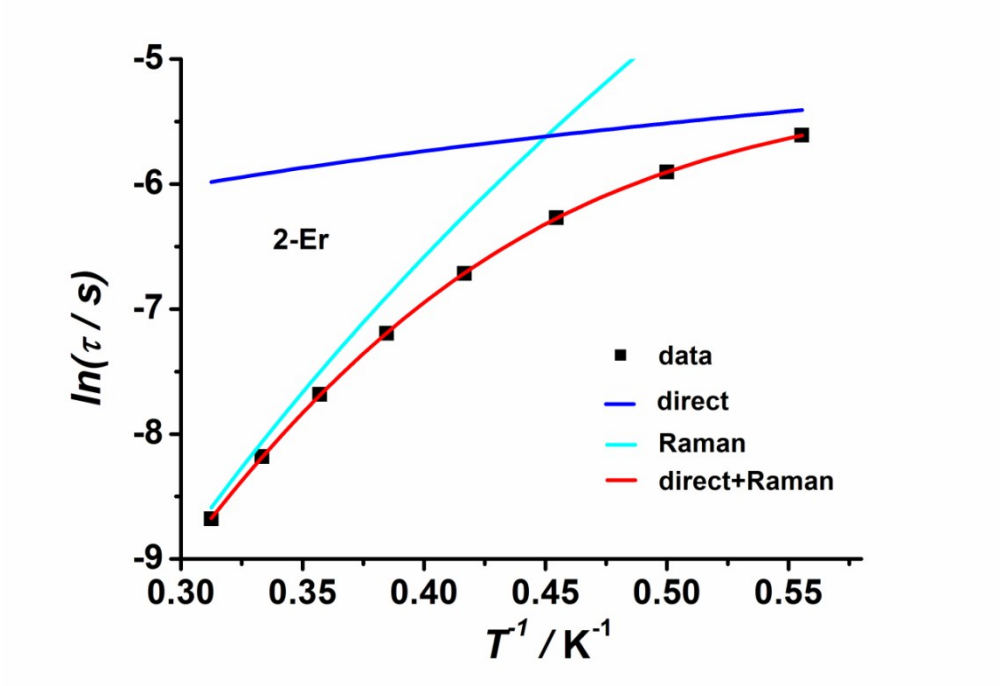

Figure S14. Temperature dependence of the magnetization relaxation rates of **2-Er** under an applied dc field of 1000 Oe. The solid red lines represent the best fit by using eq (2). The other solid lines represent data fits using individual direct (blue) and Raman (cyan) processes, respectively.

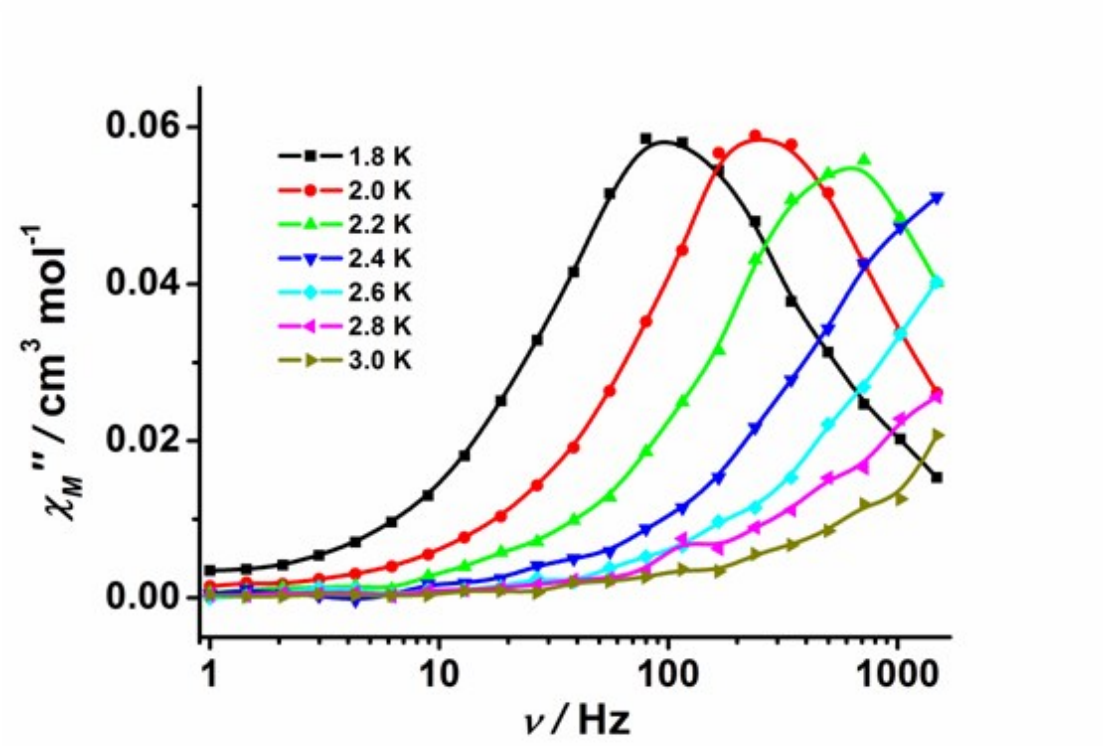

Figure S15. Frequency dependence of out-of-phase ac susceptibility (χ_M'') from 1.8 to 3.0 K under the dc field of 500 Oe for **1-Dy$_{0.18}$Y$_{0.82}$**. The solid lines are guides for the eye.

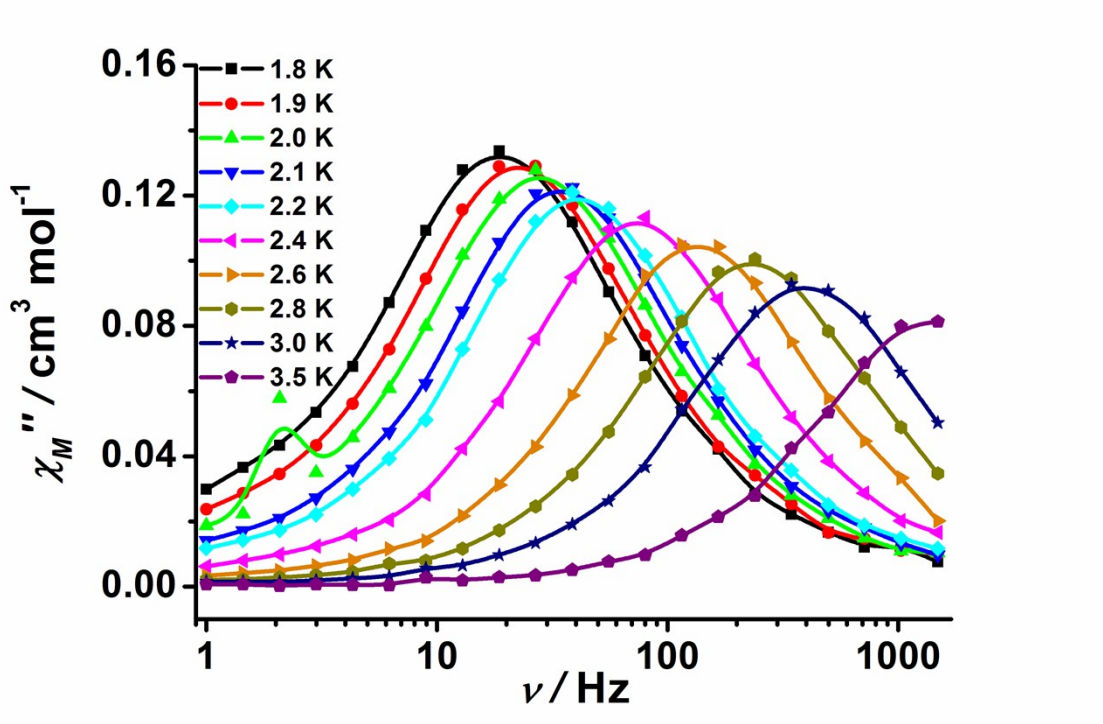

Figure S16. Frequency dependence of out-of-phase ac susceptibility (χ_M'') from 1.8 to 3.5 K under the dc field of 1000 Oe for **2-Er$_{0.13}$Y$_{0.87}$**. The solid lines are guides for the eye.

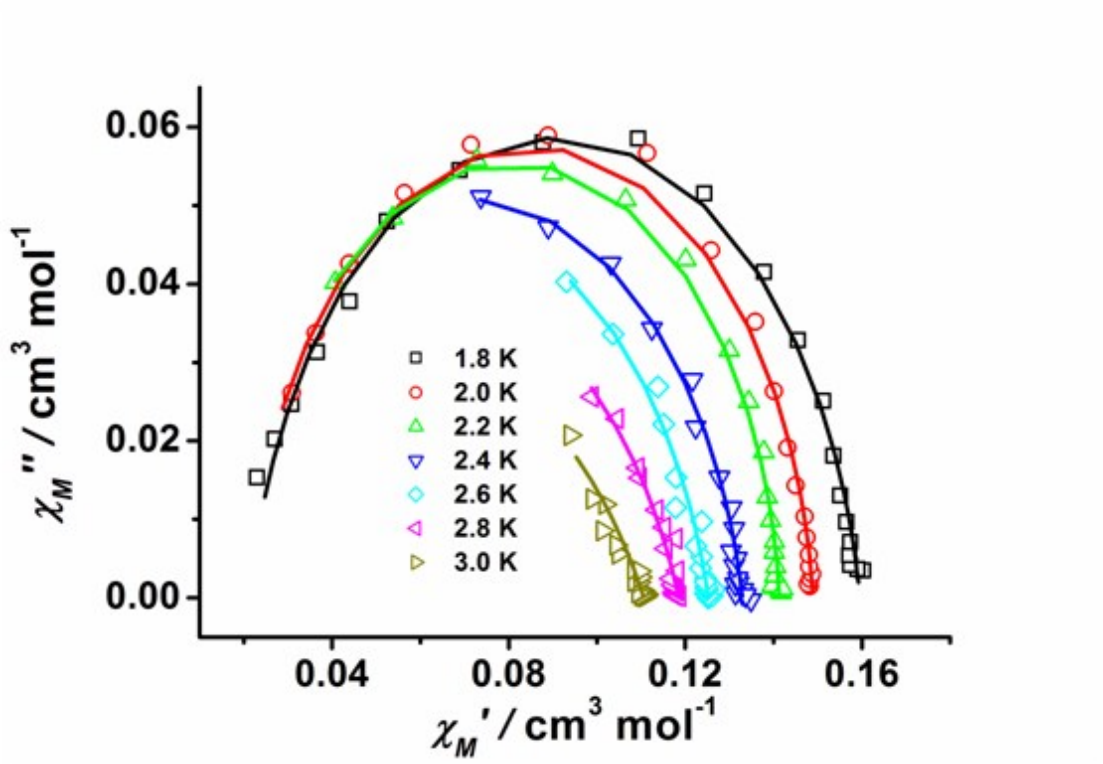

Figure S17. Cole-Cole plot obtained from the ac susceptibility data under a 500 Oe dc field in the temperature range of 1.8-3.0 K for **1-Dy$_{0.18}$Y$_{0.82}$**. Solid lines represent the best fits to a generalized Debye model.

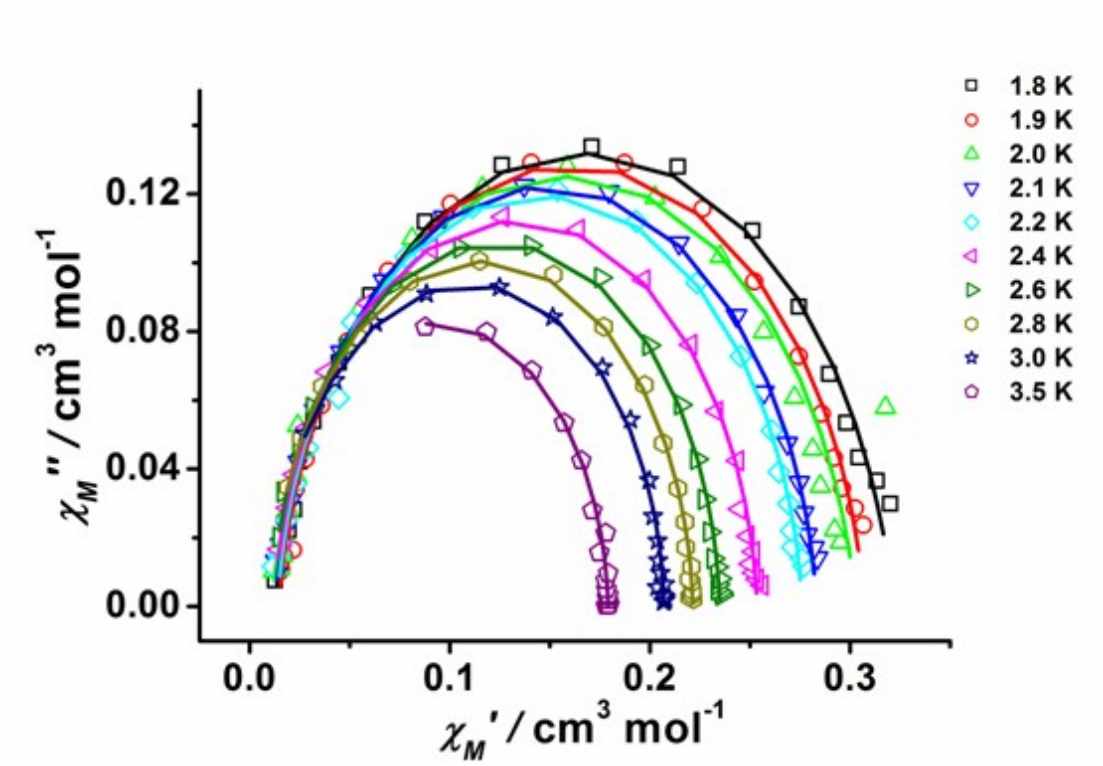

Figure S18. Cole-Cole plot obtained from the ac susceptibility data under a 1000 Oe dc field in the temperature range of 1.8-3.5 K for **2-Er$_{0.13}$Y$_{0.87}$**. Solid lines represent the best fits to a generalized Debye model.

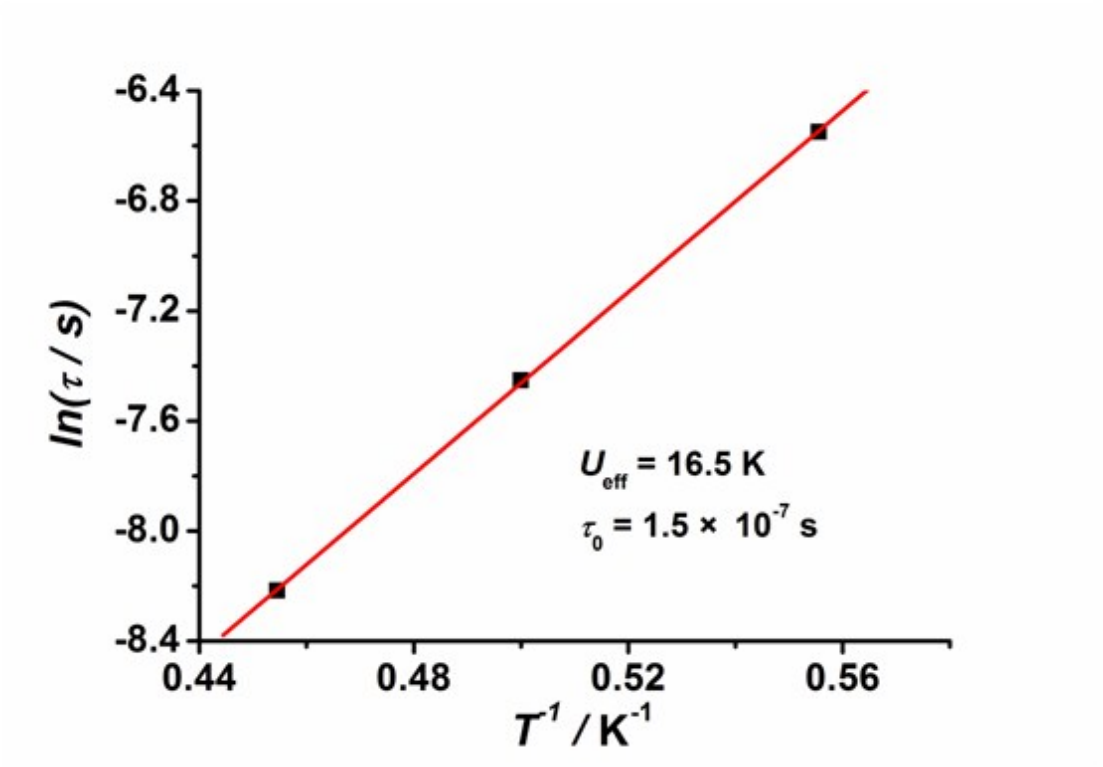

Figure S19. Relaxation time of the magnetization *ln(τ)* vs T^{-1}plots for **1-$Dy_{0.18}Y_{0.82}$**. The solid line represents Arrhenius fit.

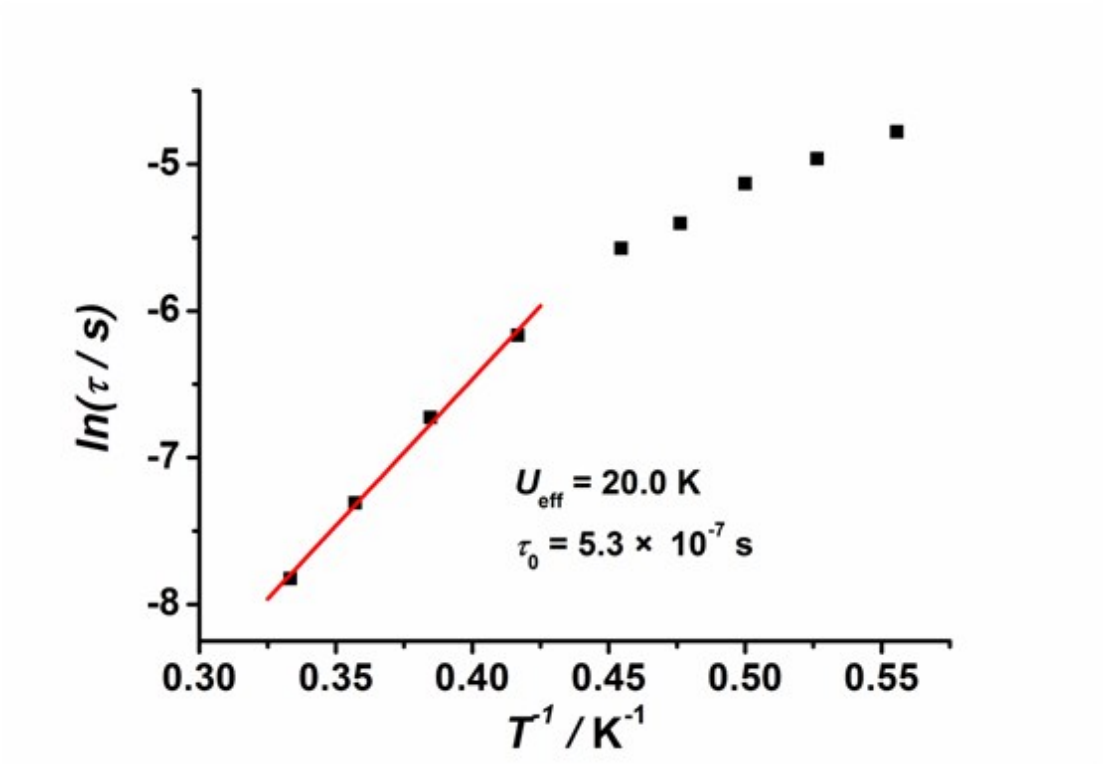

Figure S20. Relaxation time of the magnetization *ln(τ)* vs T^{-1}plots for **2-$Er_{0.13}Y_{0.87}$**. The solid line represents Arrhenius fit.

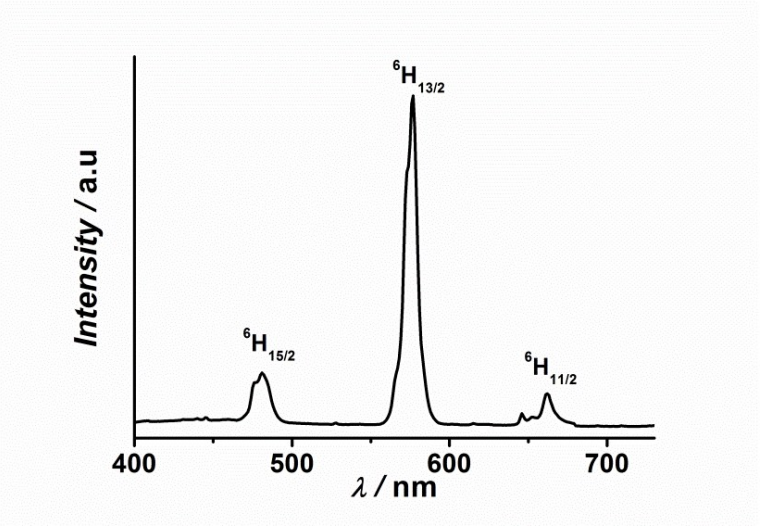

Figure S21. Emission spectrum of the complex **1-Dy** at room temperature in the solid state.

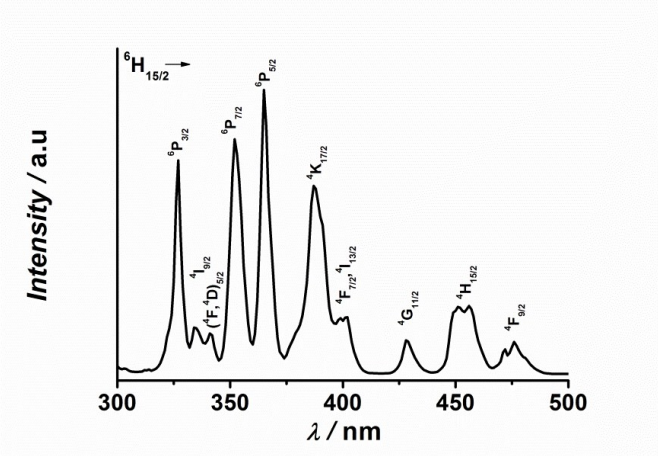

Figure S22. Excitation spectrum of the complex **1-Dy** at room temperature in the solid state.

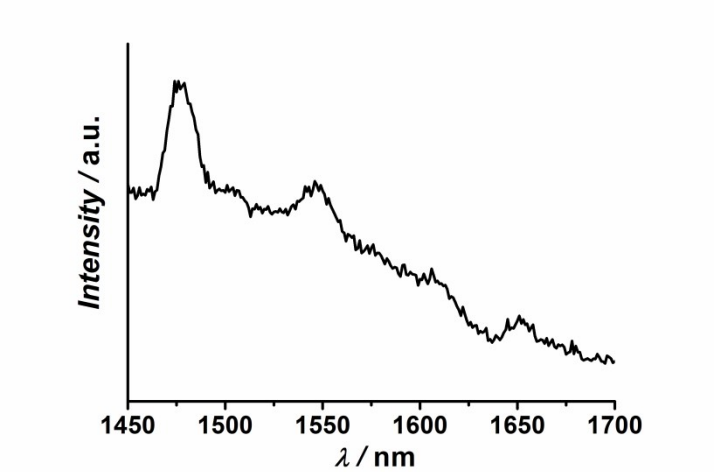

Figure S23. Emission spectrum of the complex **2-Er** at room temperature in the solid state.

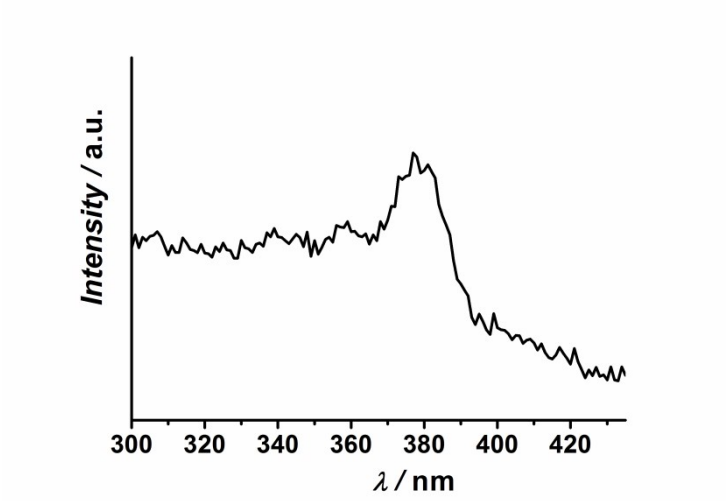

Figure S24. Excitation spectrum of the complex **2-Er** at room temperature in the solid state.